# Wide Band Microstrip Phased Array for Mobile Satellite Communications

Radha Telikepalli, *Member, IEEE*, Peter C. Strickland,
Kevin R. McKay, and Jim S. Wight, *Senior Member, IEEE*

*Abstract*—**A low profile, dual frequency, microstrip phased array has been designed and developed for INMARSAT (International Maritime Satellite organization) land mobile satellite communications. The purpose of the array was to provide a wide band coverage, right-hand circular polarization with a high gain and minimum sidelobe levels in the principal planes. The developed array has a measured frequency bandwidth of 10% with a VSWR of 1.5, a minimum gain of 12 dBic, a gain to noise temperature ratio of −8.98 dB/K, sidelobe levels 13 dB below the beam peak in both the principal planes. The size of the array was 47 cm in diameter and 1.3 cm thick including a flush mounted light weight radome with the elements and the feed lines on the same layer.**

## I. Introduction

THE phased array presented here is phase one from INMARSAT with the second phase being a scanned multiple beam array. The required array should be a right-hand circularly polarized, dual frequency antenna with a frequency range of 1530–1559 MHz for receive band, 1626.5–1660.5 MHz for transmit band, and provide a fixed elevation beam with beam peak in the middle of the required 20–60-degree coverage above horizon and be mechanically steered in the azimuth plane. The antenna has been designed to produce a gain between 12 and 13 dBic. The size of the antenna array was to be limited to a diameter of 47 cm as per the specifications. The noise temperature should be below 80 K to give a minimum gain to noise temperature ratio of −12 dB/K and the sidelobe levels should be below 13 dB in both elevation and azimuth principal planes. To reduce the sidelobe levels, the interelement spacing should be limited to $\lambda/2$ (half wavelength in each direction) which also increases the proximity of feed lines and elements that can cause degraded array performance due to high sidelobe levels and, hence, a loss of gain.

This paper presents the array design, estimated performance and measured elevation patterns, azimuth patterns, gain at the limiting frequencies of the frequency band of interest, and antenna noise temperature at the band edges of the receive band.

Manuscript received May 31, 1994; revised January 31, 1995.

R. Telikepalli and P. C. Strickland are with the CAL Corporation, Ottawa, Ontario K2H 8K7, Canada.

K. R. McKay is with the Bell Northern Research, Ottawa, Ontario, Canada.

J. Wight is with the Department of Electronics, Carleton University, Ottawa, Ontario K1S 5B6, Canada.

IEEE Log Number 9412082.

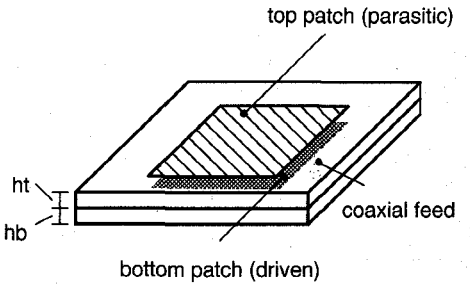


Fig. 1. Stacked configuration of the patches.

## II. Design and Development

### A. Element Development

To keep the antenna profile low, a microstrip patch array element was chosen, the shape of which depends on the beam width and space requirements. Element chosen should provide wide band performance to accommodate both transmit and receive bands. The frequency bandwidth of a microstrip patch is usually up to 5% [1] which can be improved by utilizing the effect of mutual coupling between microstrip patches in a stacked configuration. This configuration consists of two patches as shown in Fig. 1, a parasitic top element on a thicker substrate (height = $h_t$) but with the same dielectric constant as the bottom patch (height = $h_b$). It has features like fabrication simplicity, possibility of excitation with a single feed, and freedom in tuning top or bottom patches with no significant increase in the area.

Three of the elements considered for this purpose were end-shorted, circular, and square patches. Of these three, an end-shorted element has the advantage of the smallest size with the length of approximately $\lambda/4$ and a broad beam width. It was shorted at one end with the help of pins with radius, $r$ and spacing, $a$ as shown in Fig. 2. Since effective short position is sensitive to pin spacing and diameter, these parameters affect the resonant length and, hence, the frequency of the antenna. The major disadvantage was a high radiation resistance that amounts to 2.5 times that of an open-ended half wavelength square patch, a 60% reduction in radiated power, 20% higher unloaded $Q$, and hence 20% reduction in impedance bandwidth. The bandwidth was improved with the help of stacked configuration that posed fabrication difficulties due to space required to accommodate the solder for the shorting pins and difficulties encountered in tuning the bottom patch.

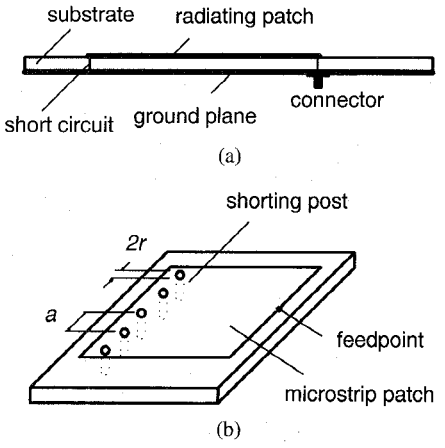


Fig. 2. End-shorted element.

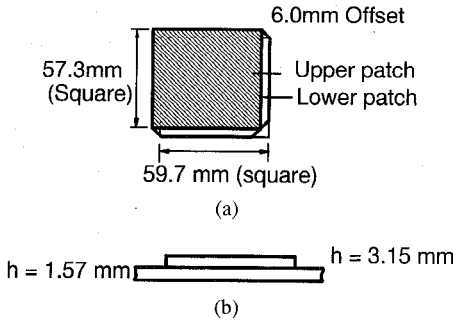


Fig. 3. (a) Front and (b) side views of the element used in the development of the array.

A circular patch and a square patch, for the same resonant frequency, possess approximately the same unloaded $Q$, efficiency, bandwidth, and the directive gain [1]; however, a square patch has the advantage of a lower profile when the elements were stacked to achieve a wide impedance bandwidth.

The element chosen for the development of the array was a stacked square patch on a substrate of $\varepsilon_r$ of 2.32 and $h = 1/16$ in. with the top patch resonating in the transmit band (1645 MHz) and the bottom patch resonating at the mid-frequency (1545 MHz) of the receive band. The impedance matching and the bandwidth was optimized by varying offset and size of the top patch that changes the coupling between the two patches. With optimized configuration shown in Fig. 3, bandwidth obtained was 10% with a VSWR of 1.5 that spreads over the entire frequency band of interest (1530–1660 MHz). Dielectric corners of the top patch were rounded to avoid the interaction with the feed lines in the array.

To achieve circular polarization, the square patch was fed at adjacent sides that excite both horizontal and vertical modes with equal amplitude. The element was fed through a Wilkinson power splitter with one arm longer than the other by $\lambda/4$ as shown in Fig. 4, which generates counterclockwise movement of electric field or right-hand circular polarization. The quality of circular polarization was tested with the axial ratio measured with a spinning dipole source and was found to be within allowable limits with a minimum value of 3.0 dB. The return loss of the element along with the hybrid is as shown in Fig. 5.

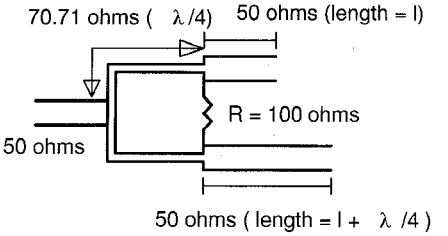


Fig. 4. Wilkinson power splitter.

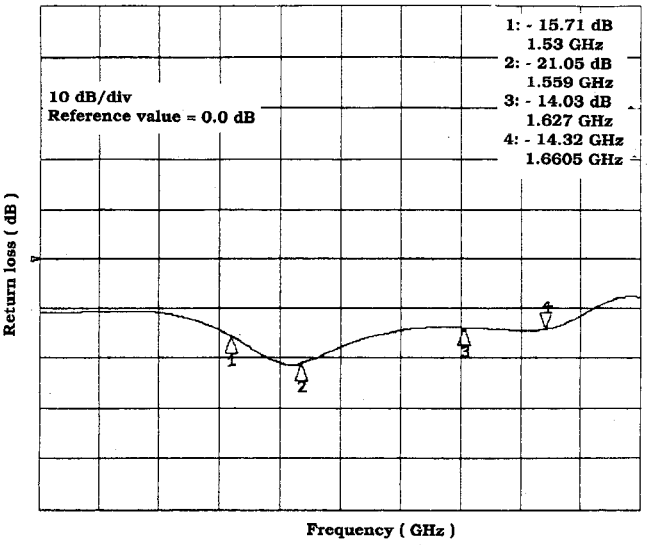


Fig. 5. Measured return loss of the microstrip element as a function of frequency.

TABLE I
REQUIRED CHARACTERISTICS OF THE ARRAY

| Parameters | Required values |
|---|---|
| Frequency bandwidth | 8.2 % |
| Position of the beam peak above horizon | around 45° |
| Peak gain (dBic) | 12 - 13 |
| Side lobe levels below the beam peak ( dB ) | -13 |
| Minimum G/T (dB/K) | -12 |

### *B. Array Design*

A 10-element array [3] was developed using the square patch designed above to suit the requirements as shown in Table I. To get the maximum directivity in the elevation plane, more number of elements were placed in this plane than those in the azimuth plane. The array produced, required radiation patterns in the principal planes, but had high unwanted grating lobes in the other planes that resulted in a power gain of 10.2 dBic minimum and can be attributed to an interelement spacing of more than $\lambda/2$ (free space wavelength being 18.8 cm at 1595 MHz). Though there was a marginal improvement with a change in the power distribution, the array was abandoned as the chosen diameter of the circular disk was able to accommodate two more elements to give more power gain.

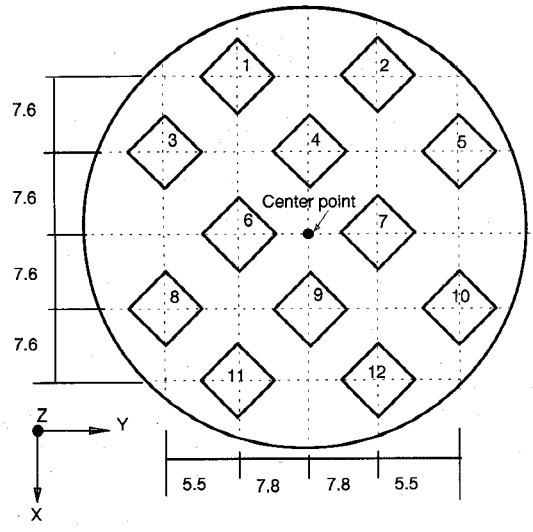


Fig. 6. Configuration of the second array (all dimensions are in cm).

TABLE II
SIMULATED AMPLITUDE AND PHASE DISTRIBUTIONS OF THE ARRAY

| Element # | Amplitude Weighting (Linear) | Phase coefficient (degrees) |
|---|---|---|
| 1 | 0.5 | 0.0 |
| 2 | 0.5 | 0.0 |
| 3 | 0.577 | - 129.0 |
| 4 | 0.577 | - 129.0 |
| 5 | 0.577 | - 129.0 |
| 6 | 1.0 | - 258.0 |
| 7 | 1.0 | - 258.0 |
| 8 | 0.577 | - 387.0 |
| 9 | 0.577 | - 387.0 |
| 10 | 0.577 | - 387.0 |
| 11 | 0.5 | - 516.0 |
| 12 | 0.5 | - 516.0 |

The second array consisted of 12 elements arranged with reduced interelement spacing, retaining the same total diameter of the array. The coordinate system was so chosen that the $x$-$y$ plane was in the same plane as the paper and the $z$ axis was orthogonal to it, away from the paper, as illustrated in Fig. 6.

Approximate array pattern was computed using the pattern multiplication theorem given by (1) [4], [5]

$$\text{Array pattern} = \text{Element pattern} \times \text{Array factor} \quad (1)$$

where the array factor determines the characteristics of the array depending upon the geometry and interelement spacing and is given by

$$\text{Array factor} = \sum_{n=1}^{N} I_n \exp\{jk(x_n \sin\theta \cos\theta + y_n \sin\theta \sin\phi) + j\beta_n\} \quad (2)$$

where $N, (x_n, y_n), I_n, \beta_n$ correspond to the total number of elements (which, in this case is 12), $x$ and $y$ coordinates of the array, linear amplitude weighting factor, and required phase delay or phase coefficient of the $n$th element. Measured element pattern was taken for this purpose to avoid modeling errors. A computer program has been developed to predict the patterns, directivity, and antenna noise temperature.

To reduce the complexity of the above expressions, amplitude coefficients of the elements were chosen symmetrically

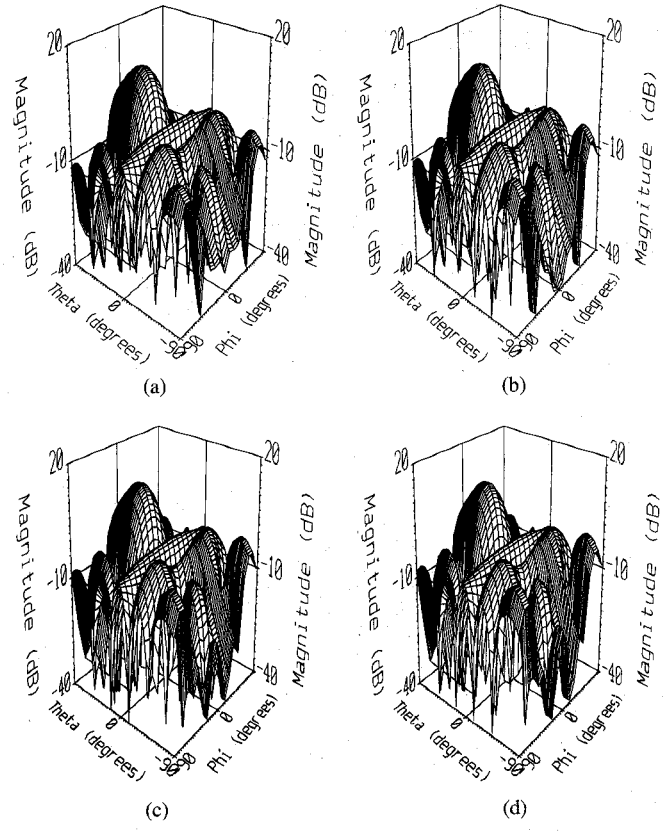


Fig. 7. Simulated radiation patterns in elevation plane; (a) 1530 MHz, (b) 1559 MHz, (c) 1627 MHz, and (d) 1660 MHz.

around the center of the array with $I_1 = I_2 = I_{11} = I_{12}, I_3 = I_4 = I_5 = I_8 = I_9 = I_{10}, I_6 = I_7$ where the elements were numbered as shown in Fig. 4. Amplitude distribution chosen was not uniform since a uniform distribution is more likely to result in high side lobe levels and, hence, an amplitude taper of $2:1:0.5\{(I_6^2+I_7^2=2),(I_3^2+I_4^2+I_5^2=1),(I_1^2+I_2^2=0.5)\}$ was used with the center elements getting the maximum power. Phase delay, also symmetrical about the center of the array, was applied to give a squinted beam in the elevation plane. Spacing between the elements was optimized using the above mentioned computer program and was found to be less than $\lambda/2$ to give the required sidelobe levels. Current optimized vertical spacing of the array is 7.6 cm, the horizontal spacing is 5.5 cm for the outer columns, and 7.8 cm for the inner two columns as shown in Fig. 6. The values of the $I_n, \beta_n$ are as shown in Table II with the three-dimensional views of elevation patterns with different frequencies as shown in Fig. 7. It can be observed that the side lobe levels did not exceed $-13$ dB in any of the planes and the patterns were found to be consistent throughout the frequency band of interest. The beam peak was modeled to be at 43 degrees above horizon with the sidelobe levels below $-13$ dB. A model array of three elements was built with the same interelement spacing as in the final array. Coupling between the adjacent elements was measured and found to give a maximum value of $-20$ dB. Similar measurements were performed with a 50 ohm line located at different distances from the patch. It was found that a separation of three dielectric thicknesses (amounts to 0.5 cm) resulted in a mutual coupling of $-25$ dB.

TABLE III
ESTIMATED LOSSES

| Losses | Values in dB |
|---|---|
| **Mismatch losses :** | |
| Hybrid | 0.11 |
| Feed | 0.18 |
| Radome | 0.05 |
| Polarization | 0.13 |
| Element | 0.18 |
| **Ohmic losses:** | |
| Feed | 0.19 |
| Hybrid | 0.10 |
| Radiating element ($\eta$ = 91.6%) | 0.38 |
| Radome | 0.05 |

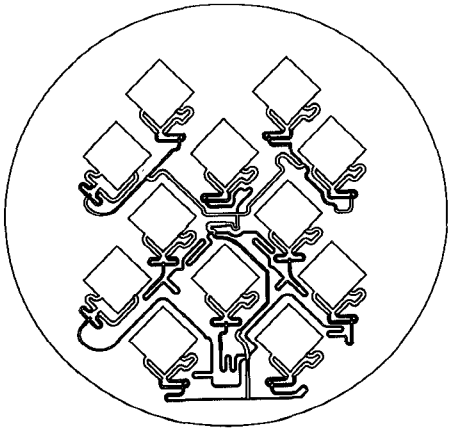

Fig. 8. Completed array configuration.

The array directivity was calculated using (3)

$$\text{Directivity} = \frac{|\boldsymbol{E}(\theta,\phi)^2|}{\frac{1}{4\pi}\int_0^{\pi}\int_0^{\pi/2} |\boldsymbol{E}(\theta,\phi)|^2 \sin\theta \, d\theta \, d\phi} \quad (3)$$

Estimated losses are shown in Table III. Efficiency of the radiating element was calculated using the dielectric and copper losses in the patch. Ohmic losses in the feed lines were minimized by using parallel feed network.

The elements were fed with the help of inlaid microstrip lines on the same board as the elements +90–degree hybrids to keep the antenna profile low. The design was carried out using Touchstone™ [6], which has a layout facility in Academy™ [6]. Power distribution was achieved with the help of impedance transformers, lengths and widths of which were calculated on Linecalc™ [6]. The required phases were supplied with microstrip lines of different lengths, the validity was tested constantly with Touchstone™ using a dispersion model which can also model the effects of sharp rounded bends used in the feed network. The phase values were verified using theoretical calculations. Distance between any two microstrip lines was kept at three times the dielectric thickness [7] to keep the mutual coupling to a minimum. The feed point was moved to a point other than the physical center of the circular

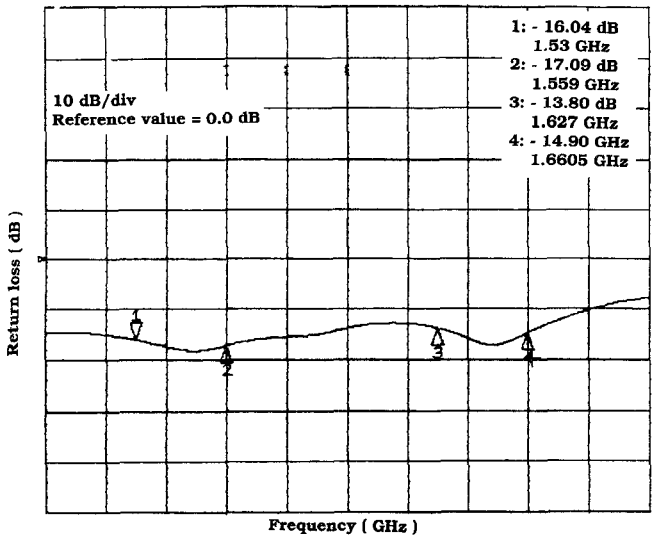


Fig. 9. Measured return loss of the array.

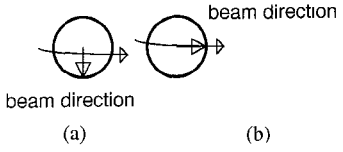


Fig. 10. Direction of beam and pattern cut. (a) Elevation pattern cut. (b) Azimuth pattern cut.

disk to accommodate the feed lines and to leave equal space around the array. The completed array is as shown in Fig. 8.

The antenna was etched on irradiated polyolefin substrate (approximately cdn $20.00/square foot) to keep the cost low and to avoid etching in the earlier stages since copper can be peeled off easily; however, the material that was used presented problems in terms of dimensional stability. A fabricated antenna was fixed to an aluminum base plate to address the above problem and to avoid any type of expansion due to extreme changes in the surrounding temperatures. Feed point of the antenna array was moved from the physical center of the antenna disk to allow uniform spacing around the antenna.

## III. MEASUREMENTS

Return loss of the array was measured to check the impedance matching and bandwidth and is as shown in Fig. 9. It can be observed that the bandwidth is 10% with a VSWR of 1.5 Arr.

ay was found to possess better matching in receive band than in transmit band.

Performance of the developed array was tested in the receive and transmit bands in terms of radiation patterns in elevation and azimuth planes (sense of direction is as shown in Fig. 10), gain and noise temperature measurements. The radiation patterns were measured with a right-hand circularly polarized helix as transmitting antenna.

Fig. 11 gives the comparison between measured and simulated elevation patterns at the beginning and end of the receive and transmit bands in the principal planes. An agreement between the mainlobes of the two can be observed in these plots. The differences in the positions of the sidelobes and nulls can be attributed to the mutual coupling even if care was

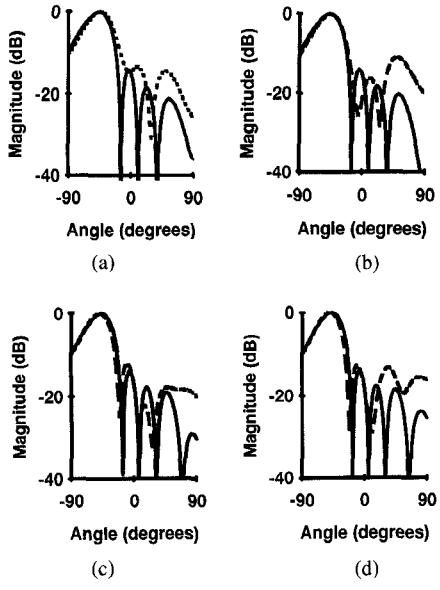


Fig. 11. Far field radiation patterns of the array in the elevation plane. Measured: (- -). Simulated: (—); (a) 1530 MHz, (b) 1559 MHz, (c) 1627 MHz, and (d) 1660 MHz.

taken in terms of spacing which, however, was not significant in the aspect that the side lobe levels were still within the design requirements.

Radiation patterns in the orthogonal plane were also measured in the same way and were compared with the corresponding simulated patterns as shown in Fig. 12. The measured beams were asymmetric about the center plane which can be attributed to movement of the feed point from the physical center of the circular disk. It can also be observed that the beams are broader by approximately 12 degrees which could have resulted in a reduction of gain, provided the side lobe levels were not lower than designed.

Power gains were measured at the beginning and end of the receive and transmit bands using a standard gain horn. The resulting gains are given in Table IV, which shows that there were some unaccounted losses in the array design.

Noise temperature was measured using the setup shown in Fig. 13 [8]. The first stage consists of determination of noise temperature of low noise amplifier (LNA) which involves measuring two power levels on spectrum analyzer with a noise source connected at the output in off (equivalent to 50 Ω load) and on states.

Let $N_{\text{on}}$ and $N_{\text{off}}$ represent the power levels when the noise source was switched on and switched off, respectively, then $Y = N_{\text{on}}/N_{\text{off}}$.

Combining this value that is called a $Y$ factor with the chart of excess noise ratio (ENR) for the noise source gives the noise figure ($F$) of LNA using

$$F = \text{ENR} - 10\ \log(Y - 1) \tag{4}$$

and the noise temperature of LNA is given by

$$T_{\text{LNA}} = T_0(F - 1) \tag{5}$$

where $T_0$ is the absolute temperature of the surroundings. The noise temperature of the antenna was measured by noting the power level with the antenna at the output when the beam

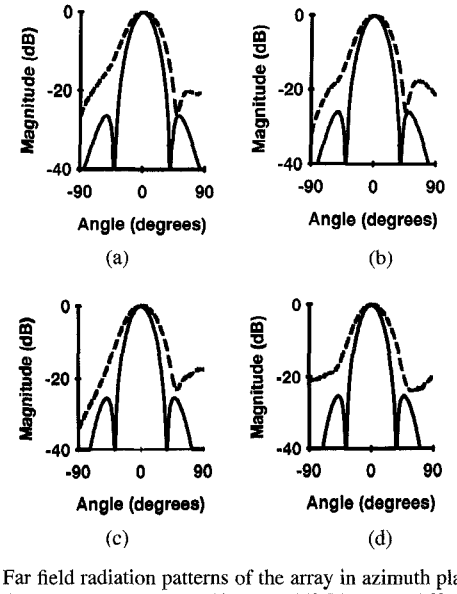


Fig. 12. Far field radiation patterns of the array in azimuth plane. Measured: (- -). Simulated: (—); (a) 1530 MHz, (b) 1559 MHz, (c) 1627 MHz, and (d) 1660 MHz.

TABLE IV
ESTIMATED AND MEASURED GAINS OF THE ARRAY

| Frequency (MHz) | Estimated (dBic) | Measured (dBic) |
|---|---|---|
| 1530 | 13.97 | 13.1 |
| 1559 | 14.05 | 13 6 |
| 1627 | 14.2 | 12.1 |
| 1660 | 14.28 | 12 3 |

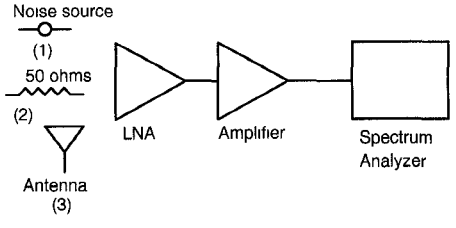


Fig. 13. Method adopted to measure antenna noise temperature.

pointing towards the sky and the power level with a 50 Ω load at the output

$$T_a = \frac{P_{\text{ant}}}{P_{\text{load}}}(T_{\text{sys}} + T_{\text{load}}) - T_{\text{sys}} \tag{6}$$

where $T_{\text{sys}} = T_{\text{LNA}}$ since there were no cable losses between LNA and antenna, load and noise source, because they were directly connected. Measured noise temperatures were found to be 51.53 K at 1530 MHz, and 70.62 K at 1559 MHz.

Receiver noise temperature was calculated by taking an LNA with noise figure of 0.5 dB ($F_{\text{LNA}} = 1.12$) and by including losses due to connector, cable, and diplexer as 0.9 dB ($F_{\text{loss}} = 1.23$), and was found to be 110 K. The expressions (7) and (8) were used to perform the above calculations

$$F_{\text{REC}} = F_{\text{loss}} + (F_{\text{LNA}} - 1)/G_{\text{loss}} \tag{7}$$

$$T_{\text{REC}} = (F_{\text{REC}} - 1)T_0. \tag{8}$$

TABLE V
MEASURED PERFORMANCE OF THE ARRAY

| Parameters | Measured values |
|---|---|
| Frequency bandwidth (%) | 10 |
| Position of the beam peak above horizon | 45° |
| Minimum peak gain (dBic) | 12.1 |
| Side lobe levels (dB below the peak) | -13.0 |
| Gain to Noise temperature ratio (dB/K) | -8.98 |

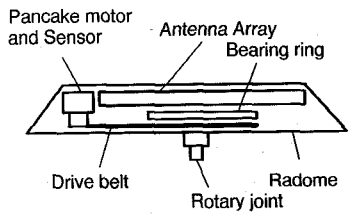


Fig. 14. Installation concept.

Combining this temperature with the measured antenna noise temperature gave $G/T$ value of $-8.98$ dB/K at the extreme frequencies of the receive band. Measured performance of the array can be understood from Table V.

The array was rotated in the azimuth plane with a pancake motor with the help of a rotary joint which is as shown in Fig. 14. It can be observed that the height of the complete assembly is only 3.5 cm and total diameter is 49 cm.

## IV. CONCLUSION

A low profile microstrip phased array was designed and developed to give a fixed beam in the middle of the required elevation angle coverage as a research and development project from INMARSAT. The array met all the design requirements with a high gain of 12 dBic, side lobe levels below $-13$ dB, frequency bandwidth of 10%, gain to noise temperature ratio of $-8.98$ dB/K.

Future work includes development of a phased array using the same element to provide multiple beams with the help of single bit phase shifters.

## ACKNOWLEDGMENT

The authors would like to thank Dr. P. Cowles, head of Antennas and Optics Group, CAL Corp., for his valuable time.

## REFERENCES

[1] K. Hirasawa and M. Haneishi, *Analysis, Design and Measurement of Small and Low-Profile Antennas*. Norwood, MA: Artech House, 1992.
[2] K. R. McKay, R. Telikepalli, P. Strickland, and J. Wight, "A compact high gain microstrip array for mobile satellite communication," *ANTEM*, 1994.
[3] K. R. Mckay, "A stacked microstrip antenna for mobile satellite communication," M.Sc.E. thesis, Carleton Univ., Ottawa, Canada, 1993.
[4] C. A. Balanis, *Antenna Theory and Practice*. New York: Harper & Row, 1982.
[5] I. J. Bhal and P. Bhartia, *Microstrip Antenna and Design*. Norwood, MA: Artech House, 1980.
[6] Trademarks of EEsof, Inc., West Lake Village, CA.
[7] Johnson and Jasik, *Antenna Engineering Handbook*. New York: McGraw-Hill, 1984.
[8] K. A. Kleinschmidt, Ed., "The ARRL handbook for radio amateur," in *American Radio Relay League*. Newington, CT, 1989.

**Radha Telikepalli** (S'92–M'93) received the Ph.D. degree in 1993 from the University of New Brunswick, Canada.

She is presently employed as an Antenna Design Engineer with CAL Corp., Ottawa, where she works on microstrip phased array antennas for mobile satellite communications using INMARSAT and MSAT. Her current research interests include numerical electromagnetics, mobile satellite communications, radio positioning systems, navigational systems, and software development in the related areas.

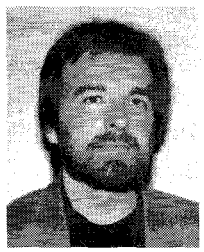

**Peter C. Strickland** received the B.Sc. degree in electrical engineering from the University of Waterloo, Ontario, Canada, the M.Sc. degree in microwave engineering from the University of Massachusetts, Amherst, and the Ph.D. degree from Carleton University, Ottawa, Ont., in 1982, 1984, and 1990, respectively.

Since 1983, at CAL Corporation he has carried out research in the area of novel microstrip antennas for navigation systems, terrestrial cellular base stations, and mobile satellite communications. He also is an Adjunct Professor at Carleton University where his current research interests is focused on medical applications of microwaves.

**Kevin R. McKay** received the B.Sc.E. degree in electrical engineering from the University of New Brunswick, Fredericton, NB, Canada, in 1990 and the M.Eng. degree in electrical engineering from Carleton University, Ottawa, Ont.,, Canada, in 1994.

He did his graduate research at CAL Corp. in the area of planar microstrip antenna arrays for mobile satellite communication from ground vehicles. He has been with Bell-Northern Research Ltd. since November 1993 as an RF/Microwave Designer of high-speed electronic modules for fiber optic transmission systems.

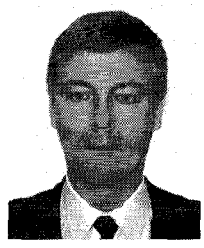

**Jim S. Wight** (S'72–M'77–SM'85) received the B.Sc. degree in 1972 from the University of Calgary, and the M.Eng. and Ph.D. degrees in 1973 and 1976, respectively, from Carleton University, Ottawa.

He is Professor and Chairman of the Department of Electronics, Carleton University. His current research interests focus on microstrip patch antennas and arrays, monolithic micorwave integrated circuits, and code synchronizers for wireless and satellite systems. He has acted for 14 years as Consultant to CAL Corp., SPAR Aerospace, Info Magnetic Technologies, and Vistar, and has conducted many joint research programs with the Communications Research Center and the Defence Research Establishment, Ottawa, over the past 20 years.